

Ruby Fluorescence Spectroscopy

Máté Garai¹, Alaa Abdelhamid¹, Vincent DiNella¹, Dr. Lily Thompson²

¹Department of Physics, The University of the South

²Department of Earth and Environmental Systems, The University of the South

High pressure research

High pressures profoundly influence physicochemical properties¹, therefore high-pressure research is applicable to material synthesis², exploring new phases of matter², understanding phase transitions³, and studying pressure-dependent properties such as elasticity⁴, sound velocities⁵, and superconductivity⁶.

High-pressure experiments are also essential for determining the properties of minerals at the extreme pressures of planetary interiors (Figure 1). This field of study, called mineral physics, provides experimental and theoretical constraints that enable scientists to determine planetary compositions, providing insights into how terrestrial bodies form and evolve through time.

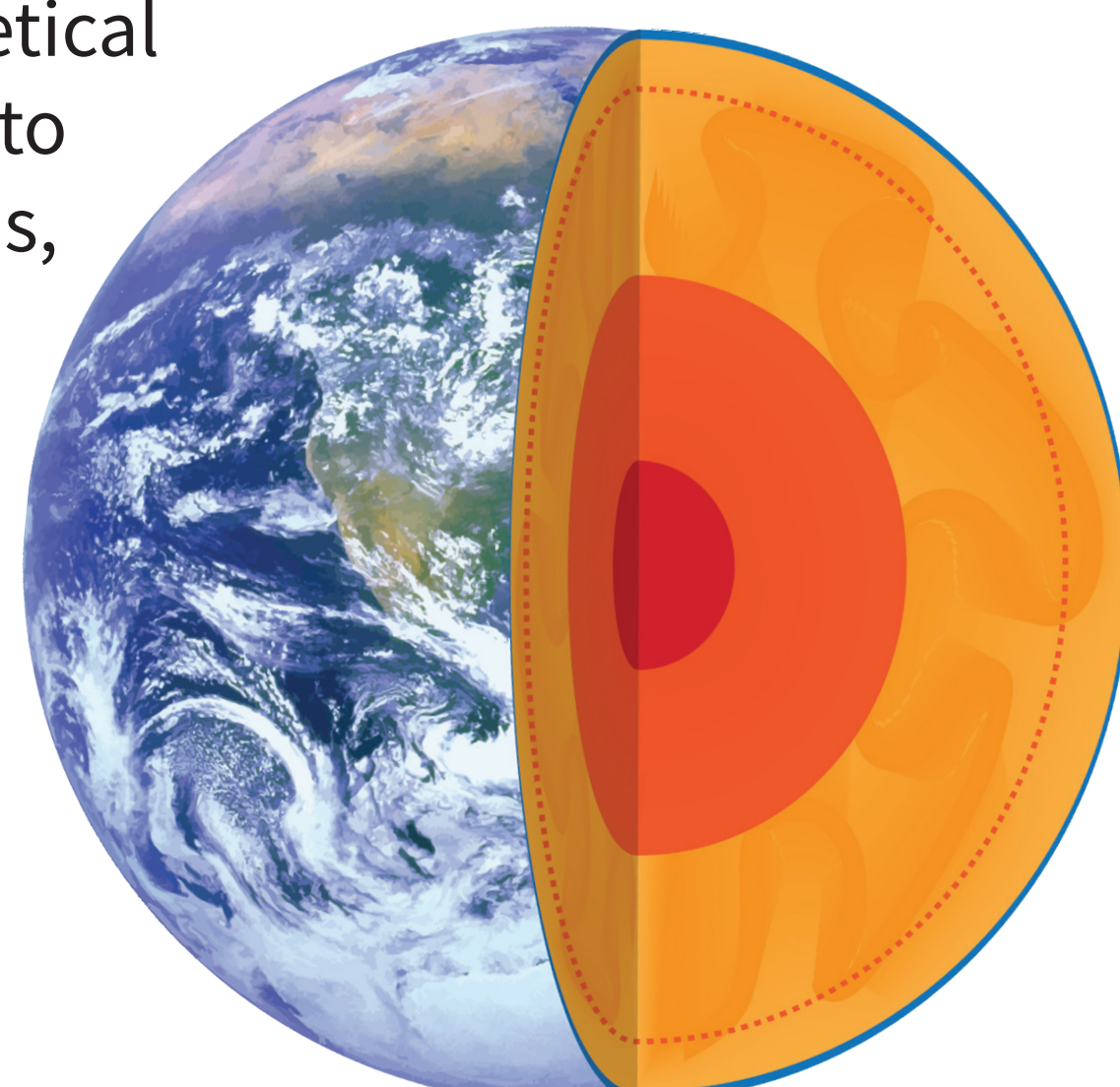


Figure 1. Layers of the Earth.

Mineral physicists use diamond anvil cells (DACs) to pressurize very small samples of geological materials (Figure 2). DACs use a pair of polished diamond anvils with parallel culets to pressurize samples, leveraging the tiny surface area of the culets and the relationship $P=F/A$ to produce extremely high pressures. Diamonds are used as anvils because they are incredibly hard and transparent, allowing researchers to optically monitor and probe the pressurized samples *in situ*.

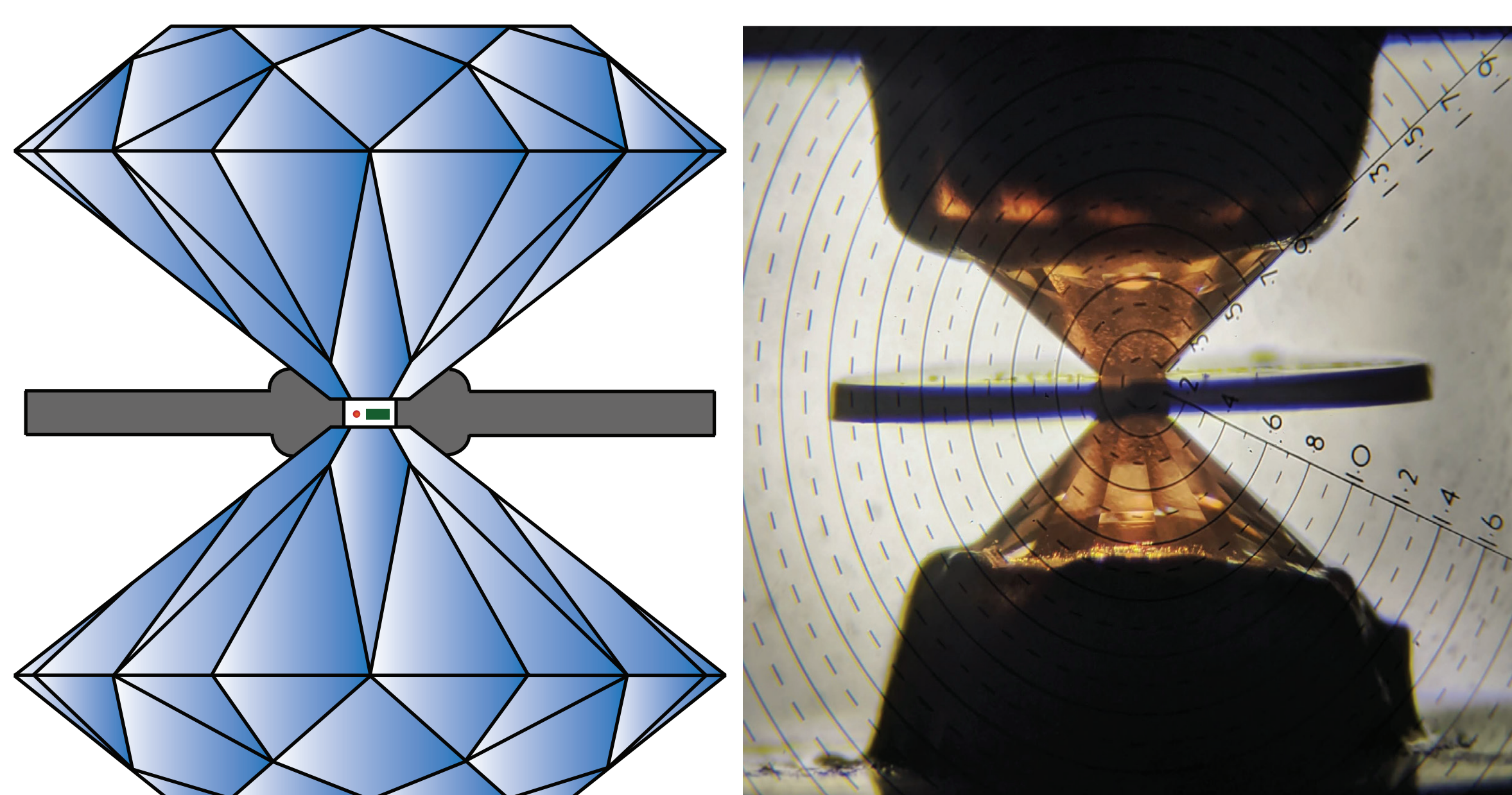


Figure 2. Diamond anvil cell schematic (left) and magnified profile photograph (right).

What is ruby fluorescence?

To measure the *in situ* pressure in DACs, we use ruby fluorescence spectroscopy (Figure 3). Fluorescence is a type of luminescence that occurs when a material absorbs a short wavelength of radiation that excites the material, and then emits radiation with a longer wavelength. When ruby (Al_2O_3 , with ~ 0.5 wt% Cr dopant) is excited by a green 532 nm laser, the Cr^{3+} ions are excited to a higher energy level, relax rapidly to two metastable energy levels, before relaxing fully to the ground state (Figures 4 and 5). The wavelength of the emitted photons is dictated by the energy difference between the metastable and ground states, and can be quantified using the peak positions in the fluorescence spectrum (Figure 6).

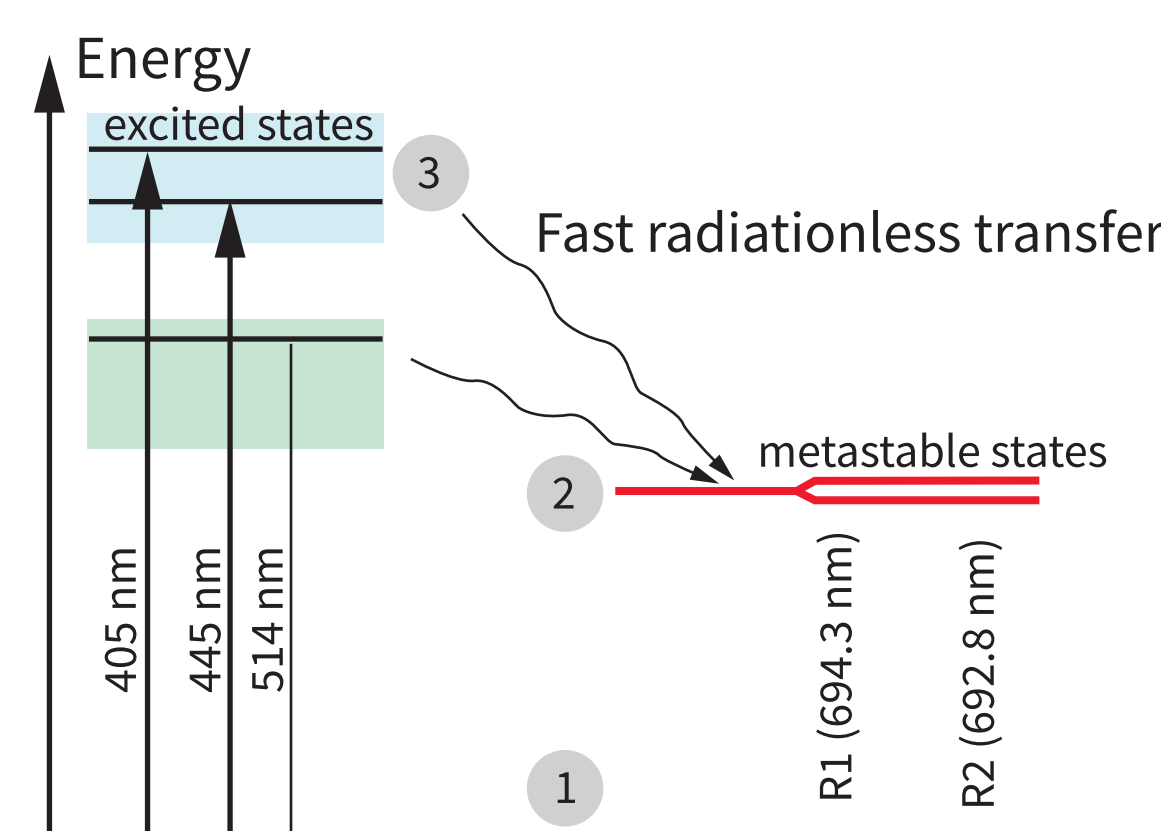


Figure 4. Ruby energy diagram.

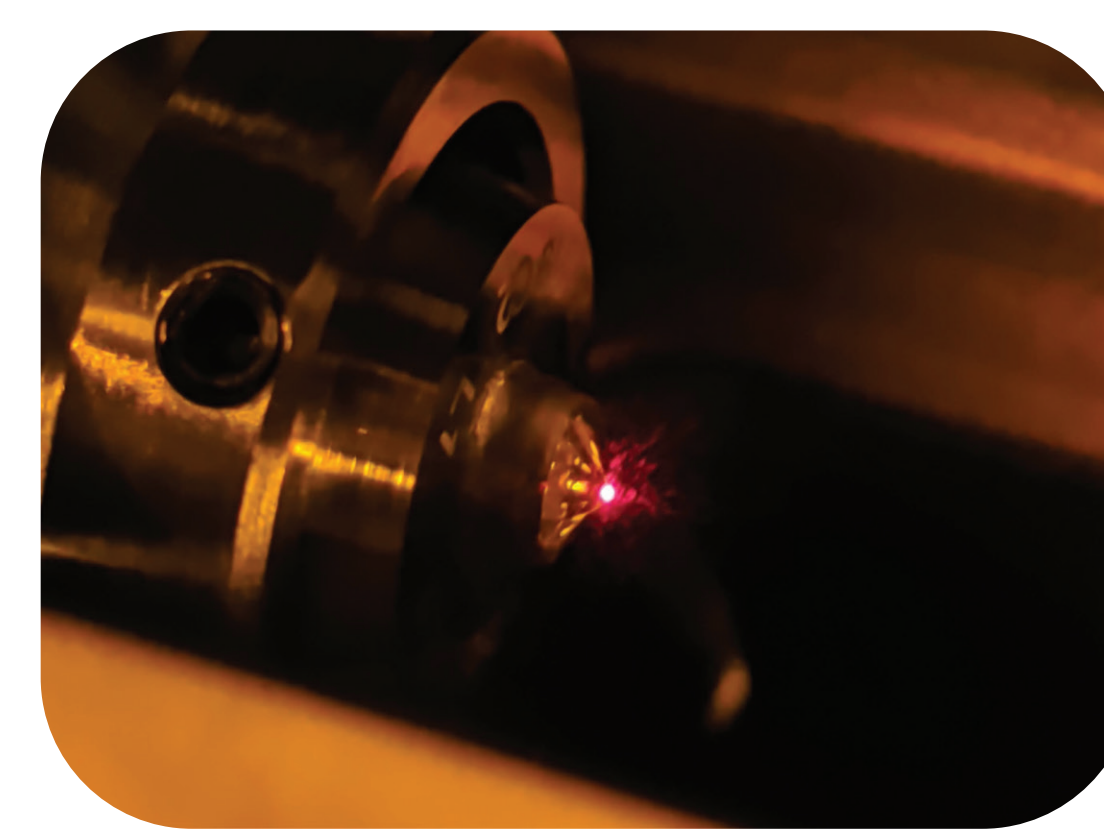


Figure 5. Excited ruby on a diamond.

At ambient conditions, the ruby fluorescence spectra has peaks at 694.3 nm (R1) and 692.8 nm (R2) (Figure 6). With increased pressure, these peaks shift to longer wavelengths in a predictable way that can be used to calculate the *in situ* pressure inside a DAC (Figure 7).

Ruby fluorescence spectra

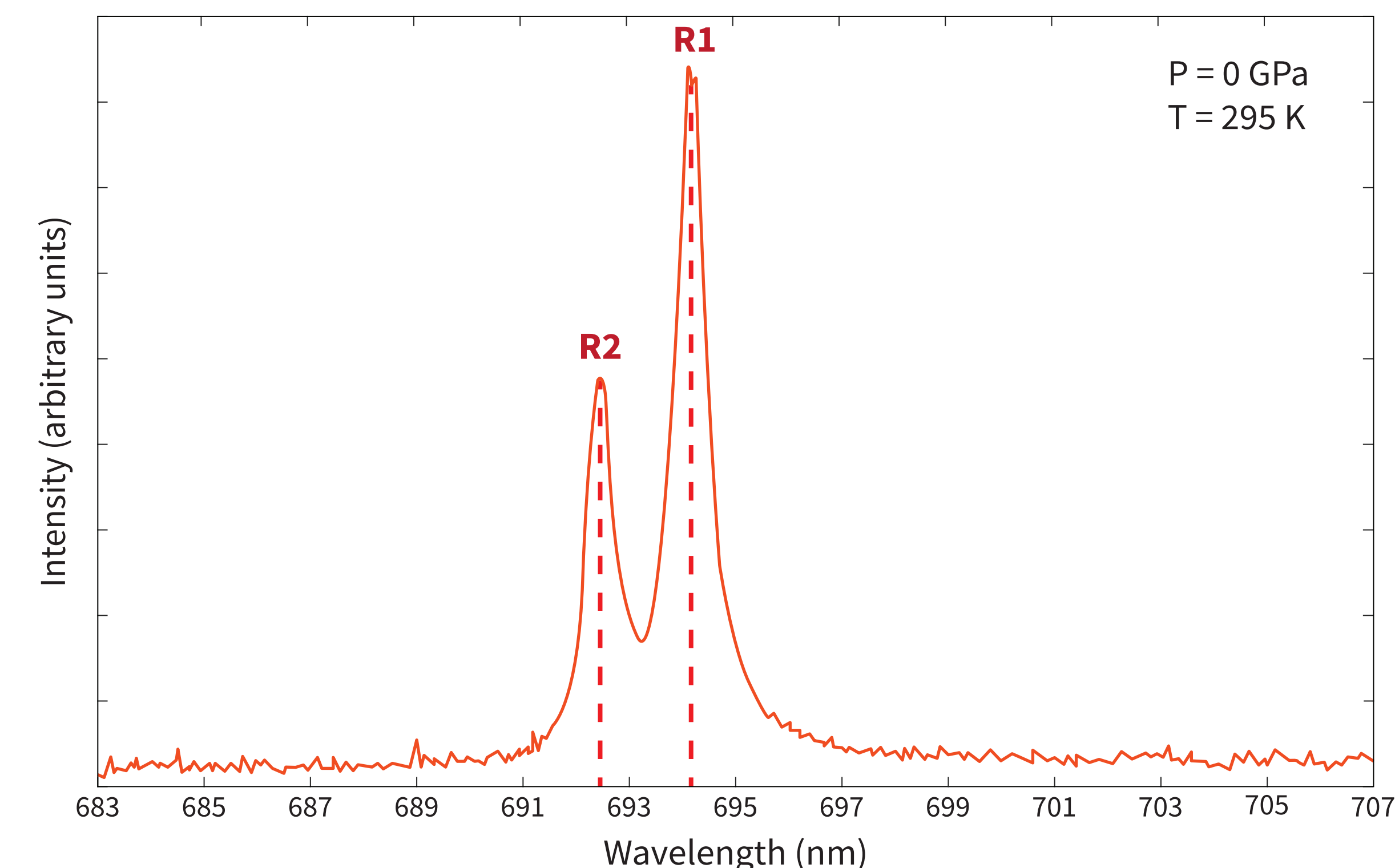


Figure 6. R1 and R2 peaks of the ruby fluorescence spectra at 1 atm.

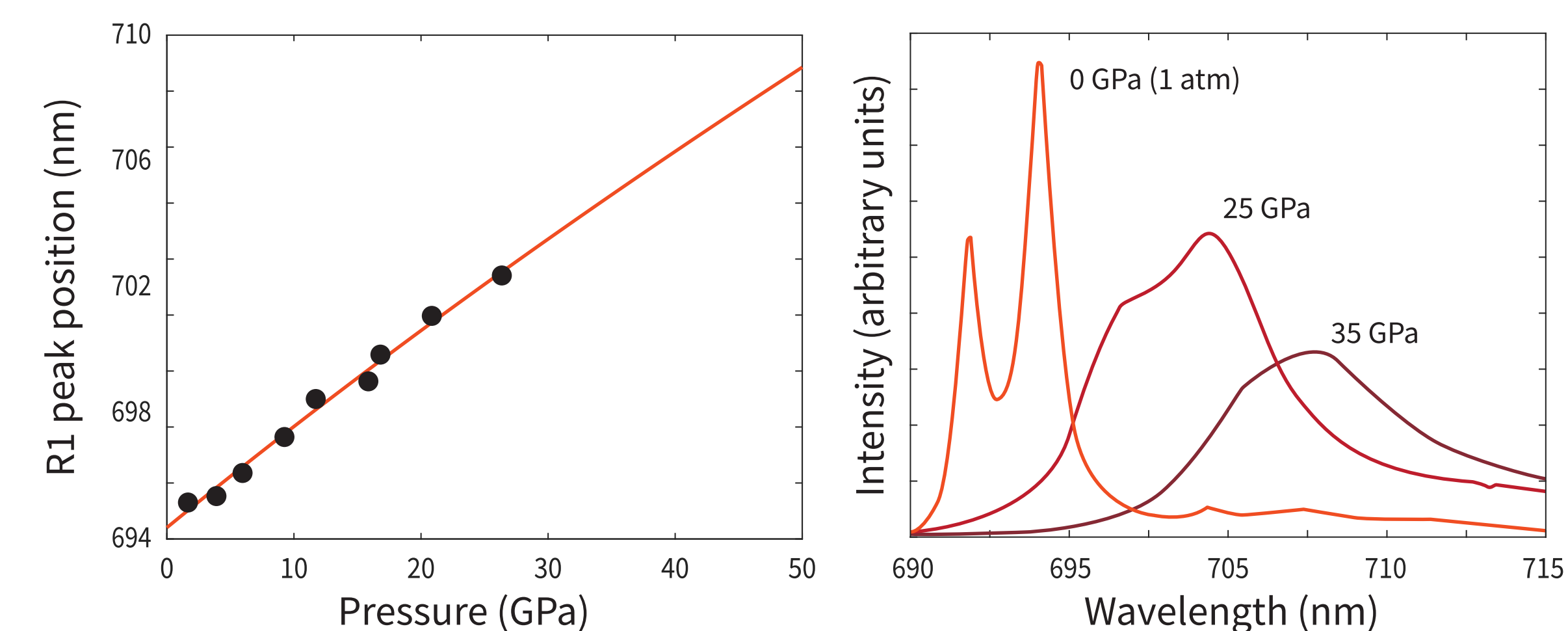


Figure 7. The R1 peak shift as a function of pressure.

Research applications

Our ruby fluorescence system (Figure 3) enables the assembly of pressurized DAC samples that can then be probed using the high flux radiation available at Department of Energy synchrotron facilities. These brilliant, collimated light sources are used to acquire high-resolution data with short collection times even for our very small samples (Figures 8 and 9). At the National Synchrotron Light Source at Brookhaven National Laboratory (Figure 10), we probed epsomite ($\text{MgSO}_4 \cdot 7\text{H}_2\text{O}$) and melanterite ($\text{FeSO}_4 \cdot 7\text{H}_2\text{O}$) in order to identify phase transitions at the temperatures and pressures of the interiors of the icy Galilean satellites where they are believed to exist.

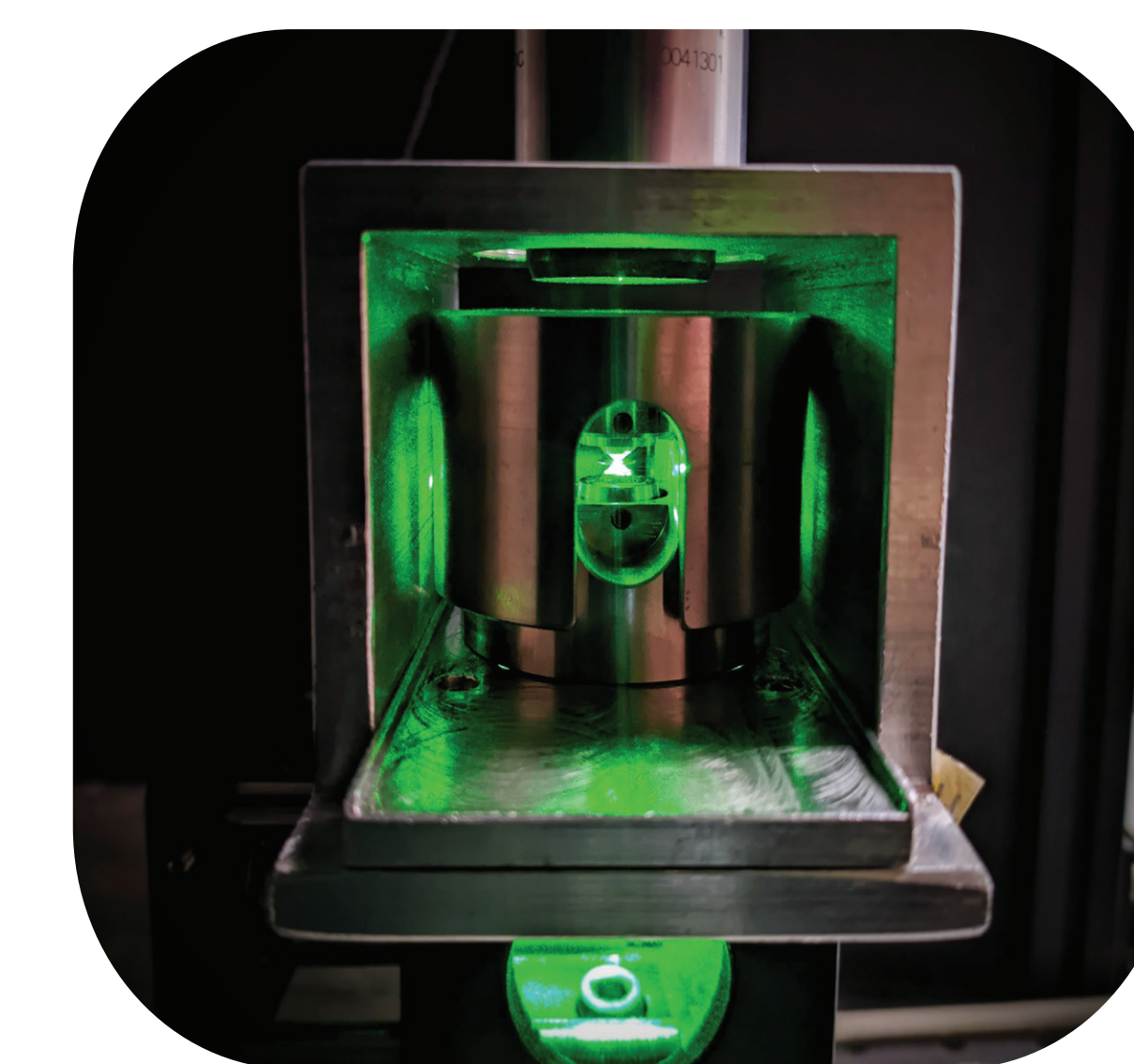


Figure 8. *In situ* Raman spectroscopy.

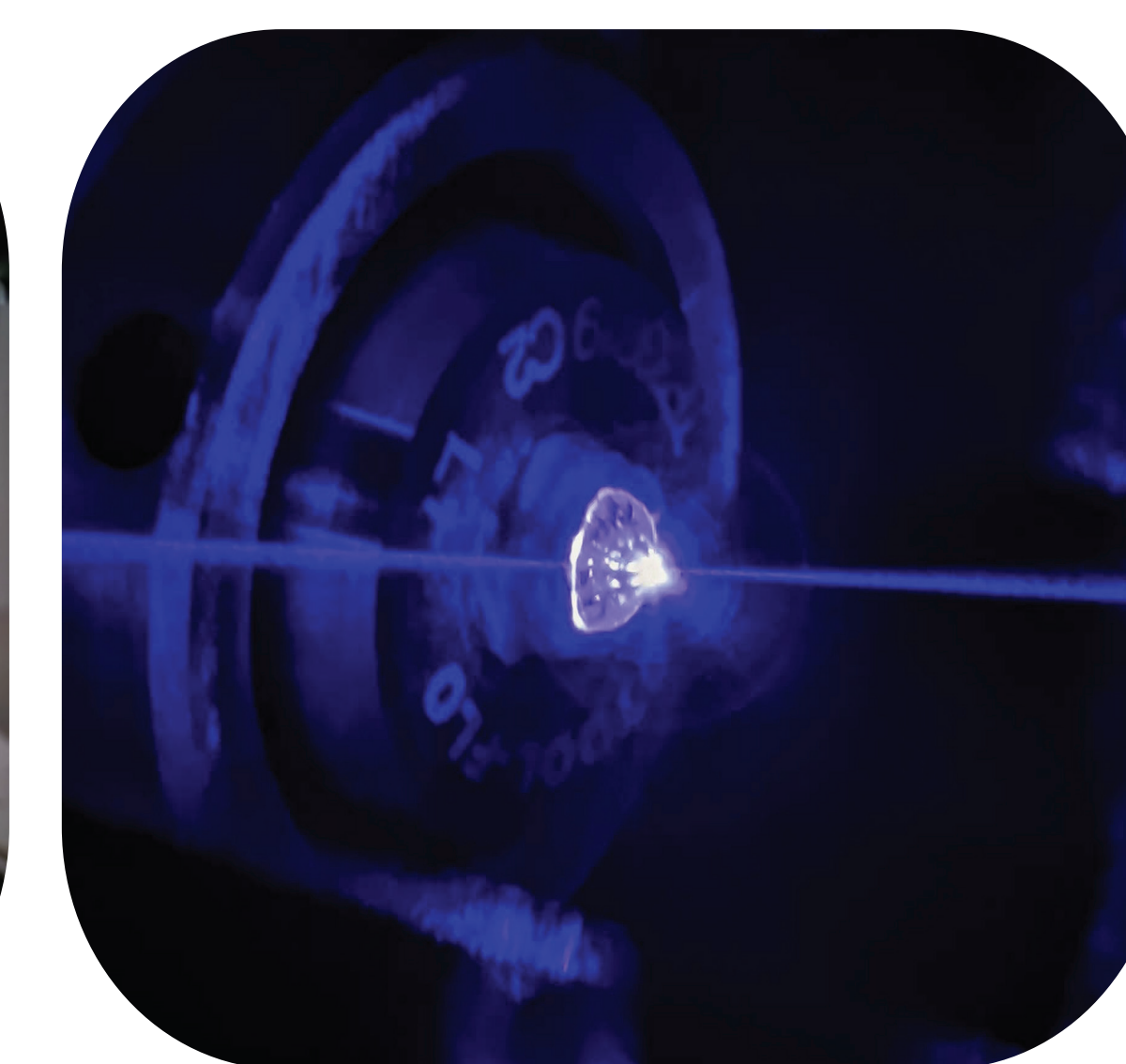


Figure 9. A 450 nm laser hitting a diamond anvil culet.

Figure 3. Ruby fluorescence spectrometer schematic diagram with optical components.

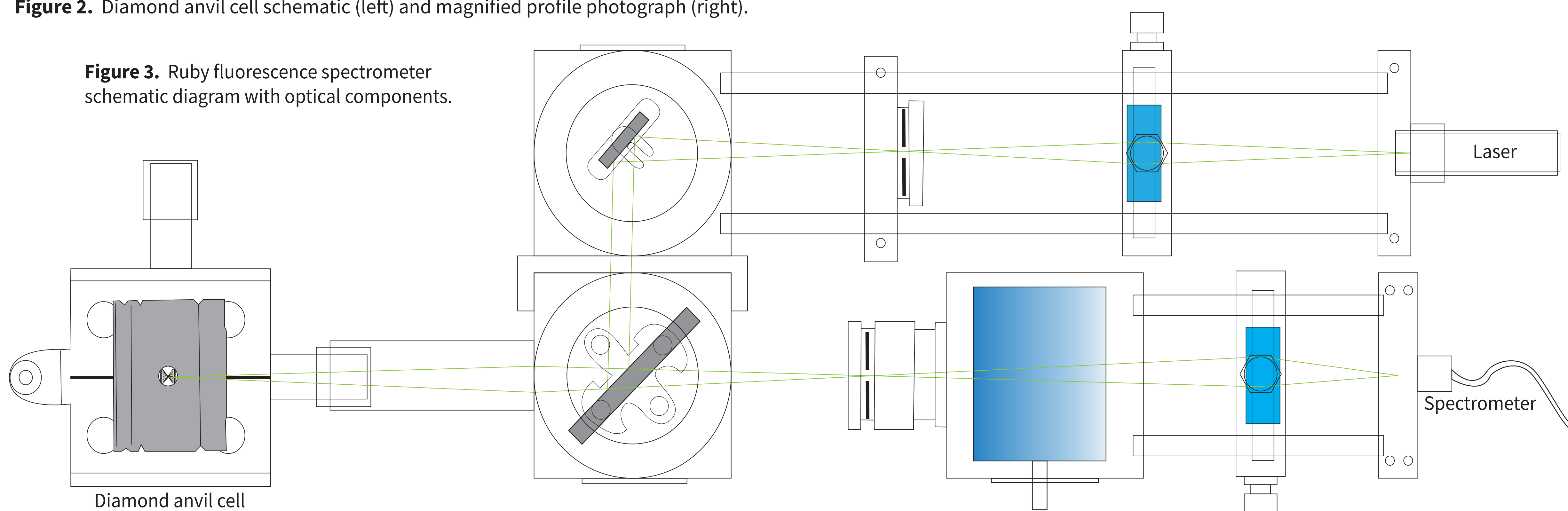


Figure 10. The National Synchrotron Light Source at Brookhaven National Laboratory.

References

- (1) Rahm et al. (2019)
DOI: 10.1021/jacs.9b02634
- (2) Millot et al. (2019)
DOI: 10.1038/s41586-019-1114-6
- (3) Dewaele et al. (2018)
DOI: 10.1038/s41467-018-05294-2
- (4) Lai et al. (2020)
DOI: 10.3791/61389
- (5) Antonangeli et al. (2015)
DOI: 10.1186/s40645-015-0034-9
- (6) Drozdov et al. (2019)
DOI: 10.1038/s41586-019-1201-8